

1 **Running title:** How do three TaGS1 perform their role?

2 **Title:** How do three cytosolic glutamine synthetase isozymes of wheat perform N
3 assimilation and translocation?

4 **Authors:**

5 Yihao Wei¹, email: yc_yihao@163.com

6 Xiaochun Wang^{1,2,3}, email: xiaochun.w@163.com

7 Telephone: 086-13783586761

8 Zhiyong Zhang¹, email: zyoung1988@126.com

9 Shuping Xiong¹, email: shupxiong@163.com

10 Yiming Zhang², email: zyiming567@163.com

11 Lulu Wang¹, email: wanglulu9501@163.com

12 Xiaodan Meng¹, email: mengxd13@163.com

13 Jie Zhang¹, email: zhangjie135239@163.com

14 Xinming Ma¹, email: xinmingma@126.com

15 Telephone: 086-13937100780

16 **Address:**

17 1. Collaborative Innovation Center of Henan Grain Crops, College of
18 Agronomy, Henan Agriculture University, Zhengzhou, China;

19 2. Department of Biochemistry and Molecular Biology, College of Life
20 Science, Henan Agriculture University, Zhengzhou, China;

21 3. State Key Laboratory of Wheat and Maize Crop Science in China, Henan
22 Agriculture University, Zhengzhou, China

23 **Submission date:** 11/8/2019

24 **The number of tables:** 1 table in text and 4 tables in supplementary data.

25 **The number figures:** 6 figures in text, Fig.2, Fig. 5 and Fig.6 are in color in print.

26 Fig.2, Fig. 3, Fig. 4, Fig. 5 and Fig.6 are in color online. 2 figures in supplementary

27 data, all are in color online.

28 **The total word count:** 6144

29 **Highlight:** Three cytosolic glutamine synthase isozymes of wheat have different role

30 and synergistically perform nitrogen assimilation and translocation.

31

32

33

34

35 **Abstract**

36 To understand how the three cytosolic glutamine synthetase (GS1) isozymes of wheat
37 (*Triticum aestivum* L., TaGS1) perform nitrogen assimilation and translocation, we
38 studied the kinetic properties of TaGS1 isozymes, the effects of nitrogen on the
39 expression and localization of TaGS1 isozymes with specific antibodies, and the
40 nitrogen metabolism. The results showed TaGS1;1, the dominant TaGS1 isozyme, had
41 a high affinity for substrates, and was widely localized in the mesophyll cells, root
42 pericycle and root tip meristematic zone, suggesting it was the primary isozyme for N
43 assimilation. TaGS1;2, with a high affinity for Glu, was activated by Gln, and was
44 mainly localized in the around vascular tissues, indicating that TaGS1;2 catalyzed Gln
45 synthesis in low Glu concentration, then the Gln returned to activate TaGS1;2, which
46 may lead to the rapid accumulation of Gln around the vascular tissues. TaGS1;3 had
47 low affinity for substrates but the highest V_{max} among TaGS1, was mainly localized in
48 the root tip meristematic zone; exogenous NH_4^+ could promote TaGS1;3 expressing,
49 indicating that TaGS1;3 could rapidly assimilate NH_4^+ to relieve NH_4^+ toxicity. In
50 conclusion, TaGS1;1, TaGS1;2 and TaGS1;3 have different role in N assimilation, Gln
51 translocation and relieving ammonium toxicity, respectively, and synergistically
52 perform nitrogen assimilation and translocation.

53 **Key words:** assimilation, cytosolic glutamine synthetase, kinetic property,
54 localization, nitrogen, translocation, wheat

55 **Abbreviations:** GS, glutamine synthetase; NH_4^+ , ammonium; NO_3^- , nitrate; NUE,
56 nitrogen use efficiency; CDS, coding sequence; TLC, thin layer chromatography.

57

58 **Introduction**

59 Wheat (*Triticum aestivum* L.) is one of the three main cereals cultivated
60 worldwide. Nitrogen (N) is an important limiting factor for the yield and quality of
61 wheat, and large quantities of nitrogen fertilizers are required to attain maximal
62 growth and productivity (Kaur *et al.*, 2015; Kichey *et al.*, 2006). To increase crop
63 production in line with human population growth, nitrogen fertilizers are being
64 applied excessively, leading to severe nitrogen pollution on a global scale (Kant *et al.*,
65 2010; Robertson and Vitousek, 2009). Therefore, there is a need to improve nitrogen
66 use efficiency (NUE) to make agriculture more sustainable (Kant *et al.*, 2010;
67 Thomsen *et al.*, 2014).

68 In order to improve crop NUE, glutamine synthetase (GS; EC 6.3.1.2) has been
69 studied numerous times owing to its essential role in the assimilation of inorganic N
70 (Bernard *et al.*, 2008; Fuentes *et al.*, 2001; Kichey *et al.*, 2006; Martin *et al.*, 2006;
71 Nigro *et al.*, 2016; Tobin *et al.*, 1985). Understanding the physiological functions of
72 GS is crucial to modulate nitrogen metabolism and to screen for germplasm with
73 enhanced NUE (Bernard *et al.*, 2008). Plant GS is classified into two groups
74 according to its subcellular location: the cytosolic glutamine synthetase isoform (GS1)
75 and the chloroplastic glutamine synthetase isoform (GS2) (Goodall *et al.*, 2013; Sun
76 *et al.*, 2015). GS2 is encoded by a single gene and plays a clear role in assimilating
77 ammonium (NH_4^+) derived from photorespiration and nitrate (NO_3^-) reduction
78 (Wallsgrave *et al.*, 1987), while GS1 is encoded by a multigene family and plays
79 nonredundant and complex roles related to N assimilation and recycling (Bernard and
80 Habash, 2009).

81 In Arabidopsis, GS1 is encoded by five individual isogenes with distinct
82 affinities for NH_4^+ and glutamate and tissue localization as well as distinct
83 physiological functions (Guan *et al.*, 2016; Guan *et al.*, 2015; Ishiyama *et al.*, 2004b;
84 Konishi *et al.*, 2017; Lothier *et al.*, 2011; Moison *et al.*, 2018). Phylogenetically, the

85 nucleotide and amino acid sequences of these isoforms do not cluster with GS1
86 sequences from cereals (Thomsen *et al.*, 2014). The function of Arabidopsis and
87 cereal GS1 isogenes can thus not be compared directly, highlighting the importance of
88 studying crop species to improve crop NUE.

89 Expression analyses and knockout studies of individual GS1 isogenes have
90 demonstrated that they have specific spatial distribution and play essential roles in
91 plant development and yield structure in rice (*Oryza sativa*), and maize (*Zea mays*)
92 (Thomsen *et al.*, 2014). Rice has three isogenes for *GS1* (*OsGS1;1-3*). Knockout of
93 *OsGS1;1*, which localizes to vascular tissues of mature leaves, showed severe
94 retardation in growth rate and grain filling (Kusano *et al.*, 2011; Tabuchi *et al.*, 2005).
95 Knockout of *OsGS1;2*, which localizes to surface cells of roots in an NH_4^+ -dependent
96 manner, showed a marked decrease in contents of Gln and asparagine (Asn), but
97 increase in NH_4^+ content in the root and xylem sap, indicating that *OsGS1;2* is
98 important in the primary assimilation of NH_4^+ taken up by rice roots (Funayama *et al.*,
99 2013; Ishiyama *et al.*, 2004a). Real time PCR indicated that *OsGS1;3* is mainly
100 expressed in the spikelet, indicating that it is probably important in grain ripening
101 and/or germination (Yamaya and Kusano, 2014).

102 Maize has five isogenes for *GS1* (*ZmGln1;1-5*), but only *ZmGln1-3* and
103 *ZmGln1-4* have been study so far. *ZmGln1-3* in the mesophyll cells is constitutively
104 expressed until a very late stage of leaf development, indicating a role in the synthesis
105 of Gln following NO_3^- reduction until plant maturity (Hirel *et al.*, 2005; Martin *et al.*,
106 2006). *ZmGln1-4* in the bundle sheath cells was up-regulated in older leaves,
107 indicating a role in the reassimilation of NH_4^+ released during protein degradation in
108 senescing leaves (Martin *et al.*, 2005; Martin *et al.*, 2006). Furthermore, knockout of
109 *ZmGln1-3* and *ZmGln1-3* results in reduced kernel number and kernel size,
110 respectively (Cañas *et al.*, 2010; Martin *et al.*, 2006).

111 However, it is hard to study the function of TaGS1 isozymes in the allohexaploid

112 wheat using gene knockout technology. Therefore, both the precise functions of
113 individual TaGS1 isozymes and how they perform nitrogen assimilation and
114 translocation are not clear. This makes it difficult to achieve goal of improving wheat
115 NUE. On the bases of phylogenetic studies and mapping data in wheat, ten GS cDNA
116 sequences are classified into four subfamilies denominate GS1 (a, b, and c), GS2 (a, b,
117 and c), GSr (1 and 2), and GSe (1 and 2) (Bernard *et al.*, 2008; Thomsen *et al.*, 2014).
118 We re-named GS1, GSr, and GSe genes as TaGS1;1, TaGS1;2, and TaGS1;3,
119 respectively, according to phylogenetic tree analysis (Thomsen *et al.*, 2014). TaGS1;1
120 transcript is present in the per fascicular sheath cells, increase from anthesis, and can
121 be upregulated in response to a reduction in N supply. Contrastingly, TaGS1;2
122 transcripts are confined to the vascular cells, remain at steady levels until a late stage
123 of development, and are downregulated under N starvation (Bernard *et al.*, 2008;
124 Caputo *et al.*, 2009). During leaf senescence, TaGS1;1 and TaGS1;2 are the
125 predominant isoforms, suggesting major roles in assimilating ammonia during the
126 critical phases of remobilization of nitrogen to the grain (Bernard *et al.*, 2008). The
127 transcription level of TaGS1;3 is very low compared to other TaGS1 genes and its
128 functions are still not known (Bernard *et al.*, 2008; Caputo *et al.*, 2009).

129 Since TaGS1 genes are highly homologous and their gene products were
130 indistinguishable at the protein levels by GS antibodies, previous studies about
131 individual TaGS1 isozyme only focus on the transcription level (Bernard *et al.*, 2008;
132 Caputo *et al.*, 2009; Goodall *et al.*, 2013; Zhang *et al.*, 2017). However, as an enzyme,
133 GS catalytic activity requires a process going from DNA, mRNA, and protein to
134 subunit assembly into holoenzymes. The regulation of each step of these processes
135 will affect the GS activity (Thomsen *et al.*, 2014). Therefore, studying the localization
136 and expression pattern of individual GS isozyme at the protein level will be more
137 conducive to understanding its function. Studies on the kinetic properties of individual
138 GS isozymes in Arabidopsis and rice showed that the affinity to substrates and the
139 ability to synthesize Gln significantly differed among GS isozymes (Ishiyama *et al.*,

140 2004a; Ishiyama *et al.*, 2004b). However, the kinetic properties of the individual GS1
141 isoenzymes have not been well characterized in wheat. In order to better understand
142 the precise functions of individual TaGS1 isozymes and how they perform nitrogen
143 assimilation and translocation, we studied the kinetic properties of TaGS1 isozymes,
144 the effects of nitrogen on the expression and localization of TaGS1 isozymes with
145 specific antibodies, and the nitrogen metabolism. Based on these new data, we
146 discovered that three TaGS1 isozymes have different role and synergistically perform
147 nitrogen assimilation and translocation. The results of this study are expected to
148 provide directions for improving nitrogen use efficiency of wheat, which would in
149 turn, abate N pollution arising from the use of excess N fertilizers.

150 **Materials and methods**

151 **Expression of recombinant wheat GS protein in *E. coli***

152 The CDS (Coding Sequence) region of *TaGS1;1*, *TaGS1;2*, *TaGS1;3*, and *TaGS2*
153 were obtained from wheat cultivar Yumai 49, and they were respectively cloned into
154 the pET21a vector in our previous study (Gu *et al.*, 2018). The recombinant wheat GS
155 protein was induced in accordance with a method described by Gu *et al.* (2018). After
156 induction, cells were harvested by centrifugation at 5000 g for 10 min at 4 °C. The
157 pellet was suspended in breaking buffer (10 mmol/L Tris, 10 mmol/L MgCl₂, 0.05 %
158 Triton X-100, 100 µg/mL PMSF, pH 7.5) and sonicated using an ultrasonic
159 homogenizer JY92-2D (Ningbo Scientz Biotechnology Co. Ltd., Ningbo, China). The
160 lysate was centrifuged at 12000 g for 15 min at 4 °C and the supernatants were
161 collected and used for kinetic measurements. Supernatant was kept on ice until used.

162 GS abundance in the supernatant was detected using Western-blot. GS
163 polypeptides were detected using polyclonal antibodies raised against both wheat GS1
164 and GS2. The relative content of GS was estimated by grey scanning using Image Lab
165 analyzer software (Version 5.1, Bio-Rad Laboratories, CA, USA).

166 **In vitro assay of individual recombinant wheat GS isozymes activity**

167 Determination of GS enzyme activity was based on an in vitro modified
168 synthetase reaction, where the amount of produced γ -glutamyl monohydroxamate
169 (GMH) is detectable by a stop reaction (Ma *et al.*, 2005; Németh *et al.*, 2018).

170 The crude extract of wheat GS protein recombinant *E. coli* was added into 800
171 μ L Reagent buffer. The reaction mixture was incubated at 25 °C for 15 min,
172 terminated by adding 800 μ L stop solution (123 mM FeCl₃, 49 mM trichloroacetic
173 acid, and 217 mM HCl) after centrifuging at 12000 g for 5 min, and the absorbance of
174 supernatants at 540 nm was determined. Reagent buffer always contained 40 mM
175 magnesium sulfate and basically 100 mM imidazole, 50 mM ATP, 40 mM
176 hydroxylamine, and 50 mM Na-glutamate but concentrations varied depending on the
177 actual kinetic assay (i.e., Na-glutamate: 0–120 mM; glutamine: 0–60 mM;
178 hydroxylamine: 0–80 mM).

179 **Design and preparation of antibodies against individual wheat GS isozymes**

180 DNA Star was used to compare the amino acid sequences of TaGS1;1, TaGS1;2,
181 TaGS1;3, and TaGS2 (Fig. S1). The hydrophilic and surface accessibility and
182 antigenicity of these polypeptide sequences with low homology were analyzed with
183 Protean (Table S1). The polypeptide sequences with strong antigenic, hydrophilic, and
184 surface accessibility were selected as individual wheat GS isozymes antigenic
185 polypeptides, i.e., TaGS1;1: KDGGFKVIVDAVEKLLKHKHE; TaGS1;2:
186 EAGGYEVIKTAIEKLGKRHAQ; TaGS1;3: LSKAGLSNGK; TaGS2:
187 TLEAEALAAKLLALKV. These antigenic polypeptides were synthesized and
188 polyclonal antibodies against individual wheat GS isozymes were prepared by
189 Zoonbio (Zoonbio Biotechnology Co., Ltd., Nanjing, China). To prepare polyclonal
190 antibodies against wheat GS protein, the purified recombinant protein antigen of
191 TaGS1;1 and TaGS2 was used.

192 **Plants growth conditions and experimental design**

193 For hydroponic treatments, uniform seeds were selected, surface sterilized with

194 75 % (v/v) ethanol for 1 min, rinsed with distilled water, and then germinated in
195 culture dishes covered with wet sterilized filter paper until the seed root length was
196 about 1 cm. The uniform seedlings were transplanted to opaque containers and
197 cultivated in distilled water. The hydroponic culture was carried out in a growth
198 chamber with the following conditions: 22 °C ± 2 °C, 50 % to 70 % relative humidity,
199 a photon fluence rate of 300 μmol photons m⁻² s⁻¹, and a 16h light period. After three
200 days, the seedlings were separated and grown on a modified Hoagland nutrient
201 solution (Table S2), with NH₄⁺ or NO₃⁻ as the sole N source at concentrations of 0, 0.2,
202 2, 5, 10, and 20 mM. Each container contains 10 plants with 0.5 L nutrient, which was
203 replaced every 3d. After 12 days, the shoots and roots were harvested individually and
204 immediately frozen in liquid nitrogen, then stored at -80 °C for further experiments. In
205 parallel, leaves and roots were selected, and immediately immersed in fixative for the
206 immunolocalization studies.

207 **RNA Isolation and quantitative real-time PCR**

208 Total RNA was extracted from the plant tissue using TRIzol Reagent (Thermo
209 Scientific). The cDNA was synthesized using the Hiscript 1st Strand cDNA Synthesis
210 Kit (Vazyme). Quantitative real-time PCR (qPCR) was performed on Step One
211 Real-Time PCR System (Life Technologies Corporation, CA, USA), and AceQ qPCR
212 SYBR Green Master Mix (Vazyme) for the assay. All the primers (Sangon) used are
213 shown in Table S3. The relative expression levels of the genes were calculated using
214 the TaATPases (Ta54227) and TaTEF (Ta53964) gene (Paolacci *et al.*, 2009) as
215 internal control.

216 **GS Activity Assay and Western blotting**

217 The total GS activity was measured in accordance with a method described by
218 Ma *et al.* (2005). Soluble protein content was determined by the Coomassie blue
219 dye-binding method using bovine serum albumin as a standard.
220 Native-polyacrylamide gel electrophoresis (PAGE) and in-gel GS activity staining

221 were performed as previously described (Zhang *et al.*, 2017). Western blotting was
222 performed in accordance with a method described by Wei *et al.* (2018). The dilution
223 ratio of antibody applied to the membrane is indicated in the figure legends.

224 **Metabolite Analysis**

225 Amino acid, ammonium, and nitrate were determined according to Wei *et al.*
226 (2018). Total N content determined using SEAL AutoAnalyzer 3 continuous flow
227 analytical system (Bran + Luebbe, Hamburg, Germany), in accordance with the
228 manufacturer's instructions. Soluble sugar was determined using the anthrone
229 colorimetric method (Tang, 1999).

230 The amino acid components were analyzed with thin layer chromatography
231 (TLC). Amino acids were identified with phenol-water (3:1) as a developing solvent
232 in silica gel G plate and using 0.5 % ninhydrin n-butyl alcohol solution as the
233 visualization reagent. Total free amino acid extracted from the shoot or root tissues
234 (1.5 µg) were loaded onto each lane of the TLC.

235 **Immunolocalization using indirect immunofluorescence analysis**

236 These tissues of leaf, root and root tip were fixed in FAA fixative at least 24h.
237 Embedded in paraffin, section and immunofluorescence were prepared by Servicebio
238 (Wuhan Servicebio technology Co., Ltd., Hubei, China). Anti-TaGS1;1, anti-TaGS1;2,
239 anti-TaGS1;3, and anti-TaGS2 antibodies diluted 1:200, 1:200, 1:500 and 1:50,
240 respectively, in blocking solution.

241 **Statistics**

242 One-way analysis of variance with a Duncan post hoc test was performed using
243 SPSS version 13.0 (IBM, Chicago, IL, USA).

244 **Accession numbers**

245 The locus numbers for wheat GS cDNA are as follows: *TaGS1;1* (DQ124209),

246 *TaGS1;2* (AY491968), *TaGS1;3* (AY491970), *TaGS2* (DQ124212).

247

248 **Results**

249 **The individual wheat GS isozymes are distinguishable at the protein level with**
250 **TaGS specific antibody.**

251 The individual recombinant wheat GS protein loaded in the gel was adjusted to a
252 uniform level using polyclonal antibodies raised against wheat GS (Fig. 1A). Then,
253 the specificity of antibodies against individual wheat GS isozymes was tested. The
254 results showed that anti-TaGS1;1, anti-TaGS1;2, anti-TaGS1;3, and anti-TaGS2
255 antibodies were monospecific to TaGS1;1, TaGS1;2, TaGS1;3, and TaGS2
256 polypeptides, respectively, with an antibody dilution ratio of 1:30000, 1:30000,
257 1:10000, and 1:10000, respectively (Fig. 1A).

258 The anti-TaGS2 antibody was monospecific to TaGS2 polypeptide for only one
259 band detected at about 42 kDa when wheat stem and leaf extract were analyzed by
260 immunoblotting after SDS-PAGE; the antibodies of individual TaGS1 did not
261 cross-react against TaGS2 polypeptide, as only one band at about 39 kDa was
262 detected when wheat stem and leaf extract were analyzed by immunoblotting (Fig.
263 1B).

264 **Kinetic properties of recombinant TaGS isoforms**

265 Kinetics of GS activities of recombinant TaGS1;1, TaGS1;2, TaGS1;3, and
266 TaGS2 were plotted against the concentration of glutamate (Glu), hydroxylamine, and
267 Gln in the reaction mixture (Fig. 2). TaGS1;2 activity was significantly inhibited
268 when Glu was supplied at the concentrations higher than 6 mM (Fig. 2A), and was
269 very weak at the different concentrations of hydroxylamine when Glu was supplied at
270 the 50 mM (Fig. 2B). However, TaGS1;2 activity was not inhibited when Glu was
271 supplied at concentrations lower than 5 mM (Fig. 2D) and was significantly increased

272 at the different concentrations of hydroxylamine when Glu was supplied at the 5 mM
273 (Fig. 2E). With increasing Gln concentrations, the activities of TaGS1;3 and TaGS2
274 remained stable. Contrastingly, in the reaction mixture with 60 mM Gln, the activity
275 of TaGS1;1 and TaGS1;2 was increased to about 2 and 6 times the activity in the
276 reaction mixture without Gln, respectively (Fig. 2C).

277 The specific activities plotted against the substrate concentrations showed
278 saturation kinetics, which followed the Michaelis-Menten equations, and the kinetic
279 constants were calculated (Table 1). The four TaGS isoenzymes can be classified into
280 different groups by the affinities to substrates. TaGS1;1 ($K_m = 0.65 \pm 0.01$ mM) and
281 TaGS1;2 ($K_m = 0.87 \pm 0.01$ mM) can be classified as isoenzymes with high affinity to
282 Glu, while TaGS1;3 and TaGS2 exhibited a low affinity to Glu (K_m values; $4.13 \pm$
283 0.35 mM and 2.43 ± 0.27 mM, respectively). As for hydroxylamine, TaGS1;1 ($K_m =$
284 0.26 ± 0.02 mM) and TaGS2 ($K_m = 0.36 \pm 0.04$ mM) showed high substrate affinity
285 than TaGS1;2 ($K_m = 0.66 \pm 0$ mM) and TaGS1;3 ($K_m = 0.64 \pm 0.04$ mM).

286 The relative GS protein content of recombinant wheat GS isozymes crude extract
287 was determined by analyzing the Western-blot results using Image Lab (Fig. 2F), the
288 results showed a TaGS1;1 : TaGS2 : TaGS1;2 : TaGS1;3 ratio of 1 : 0.1 : 0.63 : 0.06.
289 Based on the relative content of different TaGS isozymes, we calculated the V_{max} of
290 each TaGS isozymes. The V_{max} of TaGS1;3 was the highest, about 10-fold, 3-fold, and
291 2-fold of TaGS1;1, TaGS1;2, and TaGS2, respectively (Table 1).

292 **Effects of nitrogen nutrition on individual TaGS gene expression**

293 The responses of GS genes to N nutrition are crucial to understand their role in N
294 metabolism. The relative abundances of the mRNA and subunit of individual GS
295 isozymes in wheat seedling were determined by real time PCR and Western blot
296 analyses.

297 *The expression pattern of individual TaGS at the transcript level*

298 The TaGS1;1 transcript was the highest among all TaGS1 genes (Fig. 3A),
299 suggesting that TaGS1;1 was the dominant TaGS1 isoform in the shoot and root. And
300 TaGS1;1 transcript was higher under 0 - 0.2 mM N supply than under 2 - 20 mM N
301 supply (Fig. 3A).

302 The TaGS1;2 transcript in the shoot was much lower than that in root, and was
303 not affected by N treatments (Fig. 3B). In the root, TaGS1;2 transcript was the highest
304 under 0.2 mM NH_4^+ supply, and decreased with increasing NH_4^+ supply (Fig. 3B).
305 However, the TaGS1;2 transcript in root did not significantly change with increasing
306 NO_3^- supply, and was significantly lower than under NH_4^+ supply (Fig. 3B).

307 The TaGS1;3 transcript increased with increasing N supply in the shoot, but was
308 very lower than that in the root (Fig. 3C). In roots, with increasing NO_3^- supply, the
309 TaGS1;3 transcript increased, but it was significantly lower than under NH_4^+ supply
310 (Fig. 3C). And the TaGS1;3 transcript in root was higher under 2 - 20mM NH_4^+ than
311 under 0.2 mM NH_4^+ supply (Fig. 3C), indicating that high NH_4^+ concentration can
312 induce the expression of TaGS1;3 in roots.

313 The TaGS2 transcript was much higher in the shoot than that in the root (Fig.
314 3D). In the shoot, TaGS2 transcript was higher under 2 - 20 mM N supply than under
315 0 - 0.2 mM (Fig. 3D). When under 2 - 20 mM N supply, the TaGS2 transcript was
316 significantly higher under NO_3^- than under NH_4^+ supply. Interestingly, when under 2 -
317 20 mM NO_3^- supply, TaGS2 transcript in the root was significantly higher than
318 without N or under NH_4^+ supply (Fig. 3D).

319 *The expression pattern of individual TaGS subunit*

320 Western blots analysis using polyclonal antibodies raised against GS of wheat,
321 showed that GS2 was the predominant isoform in the shoot and GS1 was the
322 predominant isoform in the root (Fig. 3E, F). In the shoot, TaGS2 subunit level
323 increased with increasing N supply (Fig. 3E). In the root, TaGS1 subunit decreased
324 with increasing N supply (Fig. 3F). Furthermore, TaGS2 subunit could be detected in

325 root only when NO_3^- concentration was greater than 0.2 mM, indicating that TaGS2 in
326 the root was specifically induced by high concentration NO_3^- (Fig. 3F).

327 In the shoot, TaGS1;1 subunit abundance decreased with increasing N supply,
328 becoming difficult to detect when NH_4^+ concentration was greater than 2 mM (Fig.
329 3E). In the roots, TaGS1;1 subunit decreased with increasing NH_4^+ supply but it did
330 not significantly change with increasing NO_3^- supply (Fig. 3F). Less TaGS1;2 subunit
331 was detected in the shoot while much TaGS1;2 were detected in the root. Furthermore,
332 TaGS1;2 subunit increased with increasing NO_3^- supply in the root, but it first
333 increased and then decreased with increasing NH_4^+ supply (Fig. 3E, F). The TaGS1;3
334 subunit was very low in the shoot and root, and it was higher under NH_4^+ than under
335 NO_3^- supply (Fig. 3E, F).

336 **Effects of nitrogen nutrition on GS isozymes activity and total GS activity**

337 In previous studies, the cytosolic GS1 holoenzyme was ~490 kDa, and the
338 chloroplastic GS2 holoenzyme was ~240 kDa (Wang *et al.*, 2015). Therefore, the
339 isoforms showed different mobilities in gels (GS2 > GS1). In the shoot, the activity of
340 both GS1 and GS2 isozymes could be detected, but only GS1 isozymes activity could
341 be detected in the root (Fig. 3G). GS1 activity in the shoot was significantly higher
342 under NO_3^- than under NH_4^+ supply. However, GS1 activity in the root was
343 significantly lower under NO_3^- than under NH_4^+ supply (Fig. 3G). Moreover, the GS1
344 activity in the root reached its peak at 10 mM NH_4^+ (Fig. 3G).

345 The total GS activity in the shoot was significantly higher than that in the root,
346 and the total GS activity in the root was significantly higher under NH_4^+ than under
347 NO_3^- supply, and increased significantly by high concentration NH_4^+ (Fig. 3H).

348 **Effects of nitrogen nutrition on C/N metabolite status**

349 Without N supply, the shoot growth was significantly inhibited, while the root
350 growth was significantly promoted (Table S4). The free NH_4^+ , producing by its own

351 metabolic process, was significantly higher in the root than in the shoot (Fig. 4A).
352 Soluble sugar, the main product of photosynthesis, also accumulated in the roots (Fig.
353 4B). In the root and shoot, the free amino acid (Fig. 4C), soluble protein (Fig. 4D),
354 and total nitrogen content (Table S4) were lower than those under nitrogen sufficiency,
355 showing that nitrogen assimilation was inhibited under nitrogen deficiency.

356 Under 0.2 mM NO_3^- supply, NO_3^- was preferentially accumulated in the shoot
357 (Fig. S2). With increasing NO_3^- concentration, the content of NO_3^- in the shoot and
358 root and the content of free NH_4^+ in the root gradually increased (Fig. S2 and Fig. 4A),
359 but the content of the organic nitrogen (free amino acid, and soluble protein) did not
360 show an increasing trend (Fig. 4C, D), which indicated that nitrogen was mainly
361 stored as inorganic nitrogen with increasing NO_3^- supply.

362 Under NH_4^+ supply, the content of free NH_4^+ in the root was significantly higher
363 than in the shoot and increased with increasing NH_4^+ supply (Fig. 4A), but the content
364 of organic nitrogen (free amino acid, and soluble protein) in the shoot was
365 significantly higher than in the root and increased with increasing NH_4^+ supply (Fig.
366 4C, D), suggesting that NH_4^+ was mainly stored in the root while organic nitrogen
367 was mainly stored in the shoot with increasing NH_4^+ supply.

368 Under 2 - 20 mM N supply, the content of soluble sugar in the root was higher
369 than that in the shoot under NH_4^+ supply, but it was lower than in the shoot under
370 NO_3^- supply (Fig. 4D), indicating that the root needs more carbohydrates to assimilate
371 NH_4^+ under NH_4^+ supply. From 2 to 20 mM nitrogen, the amino acids content in plant
372 under NH_4^+ supply was about 2–3 times that under NO_3^- supply and the amino acids
373 contents in the shoot gradually increased with increasing NH_4^+ supply (Fig. 4C).
374 Moreover, the soluble protein content in plant under NH_4^+ supply was significantly
375 higher than under NO_3^- supply (Fig. 4D). These results indicate that the N
376 assimilation was enhanced in NH_4^+ -fed wheat.

377 The components of free amino acid extracted from the shoot and root tissues

378 were separated with thin layer chromatography (TLC) and stained with ninhydrin, and
379 the main components were Gln, asparagine (Asn), Glu, and aspartate (Asp) (Fig. 4E,
380 G). The relative proportion of Glu and Asp in the shoot and root were significantly
381 higher under NO_3^- than under NH_4^+ supply. However, the relative proportion of Gln
382 and Asn in the shoot and root were significantly lower under NO_3^- than under NH_4^+
383 supply (Fig. 4E, G).

384 **Effect of nitrogen on the tissue localization of individual TaGS**

385 Responses of tissue localization of TaGS to N nutrition are crucial to understand
386 the role of individual TaGS in N metabolism. Without N supply, TaGS2 and TaGS1;1
387 were the main isoforms and localized in the leaf mesophyll cells and TaGS1;1 was
388 also localized in the surrounding vessels of xylem in the vein of leaf (Fig. 5A).
389 TaGS1;2 was mainly localized in the surrounding vessels of xylem while no obvious
390 TaGS1;3 was detected in the leaf (Fig. 5A). Only TaGS1;1 was detected in the
391 vascular bundles in the maturation zone of roots (Fig. 6B), but abundant TaGS1;1 and
392 TaGS1;3 were found in the meristematic zone of roots (Fig. 5C).

393 Under 5 mM NO_3^- supply, the tissue localization of individual TaGS in the leaves
394 was very similar to that without N supply, but there were more TaGS2 and less
395 TaGS1;1 in the mesophyll cells and no TaGS1;1 was detected in the surrounding
396 vessels of xylem (Fig. 5D). In the maturation zone of roots, TaGS1;1 and TaGS2 were
397 localized in the pericycle cell, and TaGS1;2 and TaGS1;3 were localized in the
398 surrounding vessels of xylem (Fig. 5E). Moreover, abundant TaGS1;1, TaGS1;3, and
399 TaGS2 were detected in the meristematic zone of roots (Fig. 5F).

400 Under 5 mM NH_4^+ supply, the tissue localization of TaGS1;1, TaGS1;3, and
401 TaGS2 in the leaves was the same with 5 mM NO_3^- supply. TaGS1;2 was localized in
402 the surrounding vessels of xylem and phloem companion cells in the leaves (Fig. 5G).
403 In the maturation zone of roots, TaGS1;1 and TaGS1;3 were localized in the pericycle
404 cells, and TaGS1;2 and TaGS2 were not detected (Fig. 5H). In the corresponding site

405 of root tips in other treatments, the supposed root tip meristem under NH_4^+ treatment
406 was full of vascular tissue (Fig. 5I). There were abundant TaGS1;2, TaGS1;3, and
407 TaGS1;1 in the endodermis, but no TaGS2 was detected (Fig. 5I). Moreover, TaGS1;2
408 was detected in the surrounding vessels of xylem in the vascular bundle (Fig. 5I).

409 **Discussion**

410 This study was conducted to improve our understanding of the function of
411 glutamine synthetases, which are critical in nitrogen metabolism in wheat, to be able
412 to provide directions of improving nitrogen use efficiency in plants. NO_3^- , as an
413 important source of nitrogen absorbed by wheat roots, was reduced into NH_4^+ in
414 leaves, and then was assimilated by GS2 in the chloroplast (Goodall *et al.*, 2013;
415 Lothier *et al.*, 2011; Sivasankar and Oaks, 1996). Previous studies showed that the
416 GS2 transcripts were in roots (Bernard *et al.*, 2008; Goodall *et al.*, 2013; Wei *et al.*,
417 2018), but it was first time for us to discover that TaGS2 peptide and transcripts in
418 wheat roots were induced by NO_3^- (Fig. 3D, F), and was localized in the pericycle
419 cells (Fig. 5E) and the meristematic zone (Fig. 5F) of roots only under NO_3^- supply,
420 which indicated that TaGS2 mainly participated in assimilation of ammonia from
421 NO_3^- reduction in the root.

422 It is important to study the enzymatic kinetics of TaGS isozymes to illustrate
423 their biological function. Our study showed that recombinant TaGS1 isozymes had
424 significantly different enzymatic kinetics. TaGS1;1 is one major isoform in wheat
425 seedling (Fig. 3A, E, F), it showed high substrate affinity for Glu and hydroxylamine
426 but its maximum reaction rate was lowest (Table 1). Previous studies showed that
427 TaGS1;1 transcripts are present in the perifascicular sheath cells (Bernard *et al.*, 2008),
428 but we found that TaGS1;1 peptide was mainly localized in the leaf mesophyll cells
429 (Fig. 5A, D, G). In the mesophyll cells, ammonium released in mitochondria during
430 photorespiration is reassimilated in the chloroplast by GS2 (Wallsgrave *et al.*, 1987).
431 Oliveira *et al.* (2002) found that overexpression of cytosolic GS1 in leaf mesophyll

432 cells seems to provide an alternate route to chloroplastic GS2 for the assimilation of
433 photorespiratory ammonium. therefore, we speculate that TaGS1;1 in mesophyll cells
434 may participate in the reassimilation of ammonium released during photorespiration.
435 In addition, TaGS1;1 was also localized in the pericycle and the meristematic zone of
436 roots (Fig. 5), suggesting that TaGS1;1 was involved in assimilating inorganic
437 nitrogen in roots and assimilating NH_4^+ from the root tip metabolism process. The
438 very wide tissue distribution and high expression of TaGS1;1 indicated that it was the
439 primary TaGS1 isozyme for N assimilation.

440 A recent study showed that *AtGln1;3*, located in the pericycle of root in the
441 Arabidopsis, is involved in xylem loading of Gln (Konishi *et al.*, 2017). But how it
442 participates in the process is unclear. In the reaction mixture with 60 mM Gln, the
443 activity of TaGS1;2 was increased to about 6 times of that without the Gln (Fig. 2C).
444 As GS catalytic product, Gln has no feedback inhibition effect on TaGS1;2, but
445 significantly enhanced the catalytic activity of TaGS1;2. Furthermore, TaGS1;2 has a
446 high affinity for Glu (Table 1), which may indicate that TaGS1;2 catalyzes rapidly the
447 synthesis of Gln, leading to the accumulation of Gln. TaGS1;2 was mainly localized
448 around the vascular tissues (Fig. 5G, I), suggesting that TaGS1;2 can promote the
449 accumulation of Gln around vascular tissues. Gln is the main translocation form of
450 plant organic nitrogen (Setién *et al.*, 2013). In wheat, Gln concentration in leaf
451 phloem sap was dozens of times higher than in leaf tissue, where it was preferentially
452 loaded into the vascular tissue for translocation (Duan *et al.*, 2000). Peeters and Van
453 Laere (1994) pointed out that Gln has an amazing reverse concentration loading
454 efficiency to vascular tissue. Therefore, it can be considered that TaGS1;2, which is
455 mainly distributed around the vascular tissues, can rapidly accumulate Gln around the
456 vascular tissues, thus promoting the reverse concentration loading of Gln to the
457 vascular tissues. TaGS1;1 activity also increased with increasing Gln concentration,
458 but far less than that of TaGS1;2 (Fig. 2C). Only when no N was supplied, TaGS1;1
459 was found surrounding vessels of xylem (Fig. 5A). These results indicate that

460 TaGS1;1 is also involved in loading Gln to the vascular tissues, but less importance
461 than TaGS1;2. TaGS1;2 activity was inhibited by higher Glu concentration (Fig. 2A),
462 indicating the reverse concentration loading of Gln may be inhibited by high Glu
463 concentration.

464 The affinity of TaGS1;3 to Glu and hydroxylamine was lower than that of
465 TaGS1;1, but it had the highest V_{\max} (Table 1), indicating that TaGS1;3 has strong
466 NH_4^+ assimilation ability. The activity of TaGS1;3 was not affected by Gln (Fig. 3C),
467 suggesting that TaGS1;3 did not participate in the reverse concentration loading
468 process of Gln. TaGS1;3 was significantly promoted by the external supply of NH_4^+
469 (Fig. 3C, E, F), and located in pericycle cells of root and leaf mesophyll cells (Fig. 5G,
470 H), indicating that TaGS1;3 mainly performs rapid NH_4^+ assimilation at high external
471 NH_4^+ concentration, which can prevent the toxicity of high NH_4^+ concentration from
472 cells. The root grows rapidly (Table S4) both under medium without N and NO_3^-
473 medium, and a large amount of TaGS1;3 was distributed in the meristematic zone of
474 roots (Fig. 5C, F), indicating that TaGS1;3 was also involved in the assimilation of
475 NH_4^+ coming from the metabolism process of rapidly growing roots.

476 Wheat grows in soils with constantly changing available N forms and
477 concentrations. Therefore, it is difficult for a single TaGS to complete all nitrogen
478 assimilation tasks. Without external nitrogen, the roots no longer absorb inorganic
479 nitrogen, resulting in soluble sugars, carbon skeletons for nitrogen assimilation,
480 accumulation in the roots (Fig. 4B). At the same time, the shoot growth was inhibited
481 due to the lack of nitrogen (Table S4), resulting in the accumulation of photosynthetic
482 products (soluble sugars) in the leaves (Fig. 4B). N stress can cause leaf senescence,
483 promoting proteolysis and N remobilization (Caputo *et al.*, 2009), but roots
484 (meristematic zone) growth was promoted significantly (Table S4) for nitrogen stored
485 in the leaves may be mobilized and translocated through the phloem to the
486 meristematic zone for root growth. During this process, ammonia released by the
487 degradation of nitrogen-containing substances in the leaves was mainly assimilated

488 into Gln by TaGS1;1 located in the mesophyll cells (Fig. 5A), and then loaded into the
489 vessels by TaGS1;1 and TaGS1;2 and distributed around the xylem vessels (Fig. 5A
490 and Fig. 6A). The xylem vessels and phloem sieve tube can exchange substances
491 (Han *et al.*, 1986), so Gln loaded into the vessels can also enter the phloem sieve tube.
492 TaGS1;1 was mainly distributed in vascular bundles (Fig. 5A) to translocate of Gln in
493 the roots. TaGS1;1 and TaGS1;3 were distributed in the meristematic zone of roots
494 (Fig. 5C), and they jointly participated in the assimilation of ammonia produced
495 during the growth and metabolism of cells (Fig. 6A).

496 When NO_3^- was supplied, it will be firstly translocated to the shoot through the
497 xylem and reduced to NH_4^+ in the chloroplast of leaves, and then be assimilated into
498 Gln by TaGS2. Some Gln remains in the leaves for leaf growth, some can be loaded
499 into xylem by TaGS1;2 and translocated to other parts through phloem (Fig. 6B).
500 However, the more NO_3^- was supplied, the more TaGS2 was induced in the leaves and
501 roots (Fig. 3D, E, F), and the more NH_4^+ was located in the roots (Fig. 4A), indicating
502 that NO_3^- reduction and assimilation occurred both in the leaves and roots. TaGS1;1,
503 TaGS1;3, and TaGS2 were found in the pericycle of maturation zone of roots, whereas
504 TaGS1;2 was mainly distributed around the xylem vessels (Fig. 5E), indicating that
505 Gln was synthesized by TaGS1;1, TaGS1;3, and TaGS2 together, and then
506 translocated to the shoot via xylem by TaGS1;2 (Fig. 6B). Most NO_3^- is translocated
507 to shoot and stored in vacuoles of mesophyll cells or directly stored in vacuoles of
508 root cells (Xu *et al.*, 2012) for a large accumulation of NO_3^- in the shoot and root (Fig.
509 S2). However, the free amino acid content was very low under NO_3^- supply (Fig. 4C)
510 and the content of Gln and Asn (i.e., the organic N translocation forms) were
511 significantly lower than under NH_4^+ supply (Fig. 4E, G), indicating that NO_3^- was the
512 most important form for nitrogen translocation and storage.

513 NH_4^+ is an important inorganic nitrogen source, but high NH_4^+ concentration
514 tends to produce NH_4^+ toxicity to plants (Wang *et al.*, 2016). NH_4^+ penetrating into
515 roots has to be immediately assimilated to Gln by GS to prevent NH_4^+ toxicity

516 (Funayama *et al.*, 2013). Growing in an environment with a large amount of NH_4^+ ,
517 plants will accumulate a large amount of ammonium (Belastegui-Macadam *et al.*,
518 2007) and maintain high levels of inorganic nitrogen assimilation in the roots to
519 protect the photosynthetic parts of the plant against ammonium toxicity (Aarnes *et al.*,
520 2007; Cruz *et al.*, 2006; Hollstein *et al.*, 2010). In our study, with the increase of NH_4^+
521 supply, NH_4^+ was accumulated in the root (Fig. 4A) and the root growth was inhibited
522 (Table S4), which allowed the carbon skeleton from the shoot to be used for NH_4^+
523 assimilation. The meristematic zone of roots stopped cell division and differentiated
524 into vascular tissue (Fig. 5I), which helped assimilate products translocation to the
525 shoot in time. During this process, a large amount of TaGS1;1, TaGS1;2, and TaGS1;3
526 distributed in the root tips consumed the carbon skeleton translocated from the shoot
527 for nitrogen assimilation (Fig. 6C), resulting in a decrease in soluble sugar content in
528 the root (Fig. 4B). A large amount of TaGS1;2 was distributed in the vascular tissue of
529 root tips (Fig. 5I), which helped to load Gln to the vascular tissue (Fig. 6C).
530 Asparagine is another main compound for N storage and translocation due to its high
531 N/C ratio and stability (Ikeda *et al.*, 2004). It is synthesized by asparagine synthase
532 (AS) by the amidation of aspartate (Asp) using Gln as amino donor (Ikeda *et al.*,
533 2004). As an excellent compound in the carbon economy of nitrogen translocation
534 from roots to shoot, Gln in the root may be transformed into Asn by AS.

535 When the external NH_4^+ exceeds the maximum amount stored and assimilated by
536 the roots, NH_4^+ may be translocated to the shoot through the xylem and assimilated in
537 the leaf. In leaves, TaGS1;1 and TaGS1;3 were distributed in the mesophyll cells (Fig.
538 5G), and they may jointly participate in the assimilation of NH_4^+ (Fig. 6). Part of Gln
539 can then be loaded into the vascular tissue by TaGS1;2, distributed in the surrounding
540 vessels of xylem and phloem companion cells (Fig. 5G), and translocated to the tissue
541 short of nitrogen (Fig. 6C).

542 Based on the above, we can conclude that TaGS1;1 is the primary TaGS1
543 isozyme for N assimilation, TaGS1;2 mainly participates in the reverse concentration

544 loading of Gln into vascular tissues, TaGS1;3 participates in NH_4^+ assimilation of root
545 tip and detoxification of NH_4^+ , and they are synergistically perform nitrogen
546 assimilation and translocation (Fig. 6). Many studies have suggested that GS1 is
547 closely related to crop nitrogen use efficiency (Funayama *et al.*, 2013; Guan *et al.*,
548 2015; Martin *et al.*, 2006; Sakurai *et al.*, 1996; Tabuchi *et al.*, 2005; Zhang *et al.*,
549 2017). However, the outcome of one GS1 overexpression has generally been
550 inconsistent (Thomsen *et al.*, 2014). Considering the synergies of the three TaGS1
551 isozymes, they should be considered simultaneously to achieve the aim of improving
552 wheat NUE.

553 **Supplemental date:**

554 **Fig. S1** DNA Star multiple alignment of wheat glutamine synthetase amino acid
555 sequences.

556 **Fig. S2** Effect of NO_3^- supply on the content of NO_3^- in the shoot and root.

557 **Table S1** The antigenicity, hydrophilic, and surface accessibility of the TaGS isoform
558 specific peptides sequence.

559 **Table S2** Composition of nutrient solution treated with different nitrogen sources.

560 **Table S3** List of primers used for qPCR.

561 **Table S4** Effect of nitrogen regimes on dry weight, fresh weight, root length, and
562 nitrogen content.

563 **Acknowledgements**

564 We thank the Modern Agricultural Technology System in Henan province
565 (S2010-01-G04) and the 13th five-year national key research and development plan of
566 China (2016YFD0300205 and 2016YFD0300609) for supporting this research.

References

Aarnes H, Eriksen AB, Petersen D, Rise F. 2007. Accumulation of ammonium in Norway spruce (*Picea abies*) seedlings measured by in vivo ^{14}N -NMR. *Journal of Experimental Botany*

58, 929-934.

Belastegui-Macadam XM, Estavillo JM, García-Mina JM, González A, Bastias E, González-Murua C. 2007. Clover and ryegrass are tolerant species to ammonium nutrition. *Journal of Plant Physiology* **164**, 1583-1594.

Bernard SM, Habash DZ. 2009. The importance of cytosolic glutamine synthetase in nitrogen assimilation and recycling. *New Phytologist* **182**, 608-620.

Bernard SM, Møller ALB, Dionisio G, et al. 2008. Gene expression, cellular localisation and function of glutamine synthetase isozymes in wheat (*Triticum aestivum* L.). *Plant Molecular Biology* **67**, 89-105.

Cañas RA, Quilleré I, Lea PJ, Hirel B. 2010. Analysis of amino acid metabolism in the ear of maize mutants deficient in two cytosolic glutamine synthetase isoenzymes highlights the importance of asparagine for nitrogen translocation within sink organs. *Plant Biotechnology Journal* **8**, 966-978.

Caputo C, Criado MV, Roberts IN, Gelso MA, Bameix AJ. 2009. Regulation of glutamine synthetase 1 and amino acids transport in the phloem of young wheat plants. *Plant Physiology and Biochemistry* **47**, 335-342.

Cruz C, Bio AFM, Domínguez-Valdivia MD, Aparicio-Tejo PM, Lamsfus C, Martins-Loução MA. 2006. How does glutamine synthetase activity determine plant tolerance to ammonium? *Planta* **223**, 1068-1080.

Duan L, He Z, Han B. 2000. Composition and Transport of Amino Acids in Wheat Plant during Grain Development. *Journal of Triticeae Crops* **20**, 17-22.

Fuentes SI, Allen DJ, Ortiz-Lopez A, Hernández G. 2001. Over-expression of cytosolic glutamine synthetase increases photosynthesis and growth at low nitrogen concentrations. *Journal of Experimental Botany* **52**, 1071-1081.

Funayama K, Kojima S, Tabuchi-Kobayashi M, Sawa Y, Nakayama Y, Hayakawa T, Yamaya T. 2013. Cytosolic Glutamine Synthetase1;2 is Responsible for the Primary Assimilation of Ammonium in Rice Roots. *Plant and Cell Physiology* **54**, 934-943.

Goodall AJ, Kumar P, Tobin AK. 2013. Identification and Expression Analyses of Cytosolic Glutamine Synthetase Genes in Barley (*Hordeum vulgare* L.). *Plant and Cell Physiology* **54**, 492-505.

Gu M, Wei Y, Jia X, Xiong S, Ma X, Wang X. 2018. Expression characteristics of glutamine synthetase of wheat in *Escherichia coli*. *Chinese Journal of Biotechnology* **34**, 264-274.

Guan M, de Bang TC, Pedersen C, Schjoerring JK. 2016. Cytosolic Glutamine Synthetase Gln1;2 Is the Main Isozyme Contributing to GS1 Activity and Can Be Up-Regulated to Relieve Ammonium Toxicity. *Plant Physiology* **171**, 1921-1933.

Guan M, Møller I, Schjoerring J. 2015. Two cytosolic glutamine synthetase isoforms play specific roles for seed germination and seed yield structure in *Arabidopsis*. *Journal of Experimental Botany* **66**, 203-212.

Han J, Wang R, Jia Z. 1986. *The transport of assimilates in plants*. Beijing: Science Press.

Hirel B, Martin A, Tercé-Laforgue T, Gonzalez-Moro MB, Estavillo JM. 2005. Physiology of maize I: A comprehensive and integrated view of nitrogen metabolism in a C4 plant. *Physiologia Plantarum* **124**, 167-177.

Hollstein M, Montesano R, Yamasaki H. 2010. Ammonium tolerance and the regulation of two cytosolic glutamine synthetases in the roots of Sorghum. *Functional Plant Biology* **37**, 55-63.

Ikeda M, Kusano T, Koga N. 2004. Carbon skeletons for amide synthesis during ammonium nutrition in tomato and wheat roots. *Soil Science & Plant Nutrition* **50**, 141-147.

Ishiyama K, Inoue E, Tabuchi M, Yamaya T, Takahashi H. 2004a. Biochemical background and compartmentalized functions of cytosolic glutamine synthetase for active ammonium assimilation in rice roots. *Plant and Cell Physiology* **45**, 1640-1647.

Ishiyama K, Inoue E, Watanabe-Takahashi A, Obara M, Yamaya T, Takahashi H. 2004b. Kinetic properties and ammonium-dependent regulation of cytosolic isoenzymes of glutamine synthetase in Arabidopsis. *Journal of Biological Chemistry* **279**, 16598-16605.

Kant S, Bi Y, Rothstein SJ. 2010. Understanding plant response to nitrogen limitation for the improvement of crop nitrogen use efficiency. *Journal of Experimental Botany* **62**, 1499-1509.

Kaur G, Asthir B, Bains NS, Farooq M. 2015. Nitrogen Nutrition, its Assimilation and Remobilization in Diverse Wheat Genotypes. *International Journal of Agriculture & Biology* **17**, 531-538.

Kichey T, Heumez E, Pocholle D, Pageau K, Vanacker H, Dubois F, Le Gouis J, Hirel B. 2006. Combined agronomic and physiological aspects of nitrogen management in wheat highlight a central role for glutamine synthetase. *New Phytologist* **169**, 265-278.

Konishi N, Ishiyama K, Beier MP, Inoue E, Kanno K, Yamaya T, Takahashi H, Kojima S. 2017. Contributions of two cytosolic glutamine synthetase isozymes to ammonium assimilation in Arabidopsis roots. *Journal of Experimental Botany* **68**, 613-625.

Kusano M, Tabuchi M, Fukushima A, *et al.* 2011. Metabolomics data reveal a crucial role of cytosolic glutamine synthetase 1;1 in coordinating metabolic balance in rice. *The Plant Journal* **66**, 456-466.

Lothier J, Gaufichon L, Sormani R, Lemaître T, Azzopardi M, Morin H, Chardon F, Reisdorf-Cren M, Avice J-C, Masclaux-Daubresse C. 2011. The cytosolic glutamine synthetase GLN1; 2 plays a role in the control of plant growth and ammonium homeostasis in *Arabidopsis* rosettes when nitrate supply is not limiting. *Journal of Experimental Botany* **62**, 1375-1390.

Ma X, Li L, Zhao P, Xiong S, Guo F. 2005. Effect of water control on activities of nitrogen assimilation enzymes and grain quality in winter wheat. *Acta Phytocologica Sinica* **29**, 48-53.

Martin A, Belastegui-Macadam X, Quillere I, Floriot M, Valadier MH, Pommel B, Andrieu B, Donnison I, Hirel B. 2005. Nitrogen management and senescence in two maize hybrids differing in the persistence of leaf greenness: agronomic, physiological and molecular aspects. *New Phytologist* **167**, 483-492.

Martin A, Lee J, Kichey T, *et al.* 2006. Two Cytosolic Glutamine Synthetase Isoforms of Maize Are Specifically Involved in the Control of Grain Production. *Plant Cell* **18**, 3252-3274.

Moison M, Marmagne A, Dinant S, *et al.* 2018. Three cytosolic glutamine synthetase isoforms localized in different-order veins act together for N remobilization and seed filling in *Arabidopsis*. *Journal of Experimental Botany* **69**, 4379-4393.

Németh E, Nagy Z, Pécsváradi A. 2018. Chloroplast Glutamine Synthetase, the Key Regulator of Nitrogen Metabolism in Wheat, Performs Its Role by Fine Regulation of Enzyme Activity via

Negative Cooperativity of Its Subunits. *Frontiers in Plant Science* doi: 10.3389/fpls.2018.00191.

Nigro D, Fortunato S, Giove SL, Paradiso A, Gu YQ, Blanco A, de Pinto MC, Gadaleta A. 2016. Glutamine synthetase in Durum Wheat: Genotypic Variation and Relationship with Grain Protein Content. *Frontiers in Plant Science* doi: 10.3389/fpls.2016.00971.

Oliveira IC, Brears T, Knight TJ, Clark A, Coruzzi GM. 2002. Overexpression of cytosolic glutamine synthetase. Relation to nitrogen, light, and photorespiration. *Plant Physiology* **129**, 1170-1180.

Paolacci AR, Tanzarella OA, Porceddu E, Ciaffi M. 2009. Identification and validation of reference genes for quantitative RT-PCR normalization in wheat. *BMC Molecular Biology* doi: 10.1186/1471-2199-10-11.

Peeters KMU, Van Laere AJ. 1994. Amino acid metabolism associated with N-mobilization from the flag leaf of wheat (*Triticum aestivum* L.) during grain development. *Plant, Cell & Environment* **17**, 131-141.

Robertson GP, Vitousek PM. 2009. Nitrogen in Agriculture: Balancing the Cost of an Essential Resource. *Annual Review of Environment and Resources* **34**, 97-125.

Sakurai N, Hayakawa T, Nakamura T, Yamaya T. 1996. Changes in the cellular localization of cytosolic glutamine synthetase protein in vascular bundles of rice leaves at various stages of development. *Planta* **200**, 306-311.

Setién I, Fuertes-Mendizabal T, González A, Aparicio-Tejo PM, González-Murua C, González-Moro MB, Estavillo JM. 2013. High irradiance improves ammonium tolerance in

wheat plants by increasing N assimilation. *Journal of Plant Physiology* **170**, 758-771.

Sivasankar S, Oaks A. 1996. Nitrate assimilation in higher plants: the effect of metabolites and light. *Plant Physiology and Biochemistry* **34**, 609-620.

Sun FF, Wang Z, Mao XY, Zhang CW, Wang DS, Wang X, Hou XL. 2015. Overexpression of BcGS2 gene in non-heading Chinese cabbage (*Brassica campestris*) enhanced GS activity and total amino acid content in transgenic seedlings. *Scientia Horticulturae* **186**, 129-136.

Tabuchi M, Sugiyama K, Ishiyama K, Inoue E, Sato T, Takahashi H, Yamaya T. 2005. Severe reduction in growth rate and grain filling of rice mutants lacking OsGS1;1, a cytosolic glutamine synthetase1;1. *The Plant Journal* **42**, 641-651.

Tang Z. 1999. *Guidelines for modern plant physiology experiments*. Beijing: Science Press.

Thomsen HC, Eriksson D, Møller IS, Schjoerring JK. 2014. Cytosolic glutamine synthetase: a target for improvement of crop nitrogen use efficiency? *Trends in Plant Science* **19**, 656-663.

Tobin A, Ridley S, Stewart G. 1985. Changes in the activities of chloroplast and cytosolic isoenzymes of glutamine synthetase during normal leaf growth and plastid development in wheat. *Planta* **163**, 544-548.

Wallsgrave RM, Turner JC, Hall NP, Kendall AC, Bright SW. 1987. Barley mutants lacking chloroplast glutamine synthetase—biochemical and genetic analysis. *Plant Physiology* **83**, 155-158.

Wang F, Gao J, Liu Y, Tian Z, Muhammad A, Zhang Y, Jiang D, Cao W, Dai T. 2016. Higher Ammonium Transamination Capacity Can Alleviate Glutamate Inhibition on Winter Wheat (*Triticum aestivum* L.) Root Growth under High Ammonium Stress. *PLOS ONE* doi:

10.1371/journal.pone.0160997.

Wang X, Wei Y, Shi L, Ma X, Theg SM. 2015. New isoforms and assembly of glutamine synthetase in the leaf of wheat (*Triticum aestivum* L.). *Journal of Experimental Botany* **66**, 6827-6834.

Wei Y, Shi A, Jia X, Zhang Z, Ma X, Gu M, Meng X, Wang X. 2018. Nitrogen Supply and Leaf Age Affect the Expression of TaGS1 or TaGS2 Driven by a Constitutive Promoter in Transgenic Tobacco. *Genes* **9**, 406.

Xu G, Fan X, Miller AJ. 2012. Plant Nitrogen Assimilation and Use Efficiency. *Annual Review of Plant Biology* **63**, 153-182.

Yamaya T, Kusano M. 2014. Evidence supporting distinct functions of three cytosolic glutamine synthetases and two NADH-glutamate synthases in rice. *Journal of Experimental Botany* **65**, 5519-5525.

Zhang Z, Xiong S, Wei Y, Meng X, Wang X, Ma X. 2017. The role of glutamine synthetase isozymes in enhancing nitrogen use efficiency of N-efficient winter wheat. *Scientific Reports* doi: 10.1038/s41598-017-01071-1.

Tables

Table 1 The kinetic properties of the wheat GS isoenzymes

	K_m^* (mM)		$V_{max}^\#$ (nKat/1 unit protein)	
	Glu	Hydroxylamine	Glu	Hydroxylamine
TaGS1;1	0.65±0.01 d	0.26±0.02 c	0.13±0.001 d	0.1±0.002 d
TaGS1;2	0.87±0.01 c	0.66±0.003 a	0.5±0.002 c	0.36±0.003 c
TaGS1;3	4.13±0.35 a	0.64±0.04 a	1.63±0.06 a	1.36±0.07 a
TaGS2	2.43±0.27 b	0.36±0.04 b	0.79±0.03 b	0.85±0.03 b

* For TaGS1;1, TaGS1;2, TaGS1;3 and TaGS2, the concentration of Glu used for curve fitting was 0-40mM, 0-5 mM, 0-120 mM and 0-120 mM, respectively; the concentration of hydroxylamine used for curve fitting was 0-80 mM, 0-50 mM, 0-30 mM and 0-80 mM, respectively. The volume of individual recombinant wheat GS isozymes crude extract, with 200 μ L of TaGS1;1, 150 μ L of TaGS1;2, 450 μ L of TaGS1;3 and 300 μ L TaGS2 were used for the GS enzyme assays.

One kat of enzyme activity was defined as 1 mol GMH synthesized per second at 25°C.

Data are means of three independent biological replicates \pm SD. The different letters above each sample indicate statistically significant differences where $P < 0.05$ according to one-way ANOVA Duncan post-hoc test.

Figure legends

Fig. 1 Cross-reactivity of anti-GS antibodies to the individual recombinant wheat GS proteins (A) and the wheat GS proteins in different tissues (B). The dilution ratio of the anti-TaGS, anti-TaGS1;1, anti-TaGS2 anti-TaGS1;2 and anti-TaGS1;3 antibody, is 1:5000, 1:30000, 1:10000, 1:30000 and 1:10000, respectively.

Fig. 2 The activity of individual recombinant wheat GS isozymes in relation to additional Glu (A), hydroxylamine (B) and Gln (C). The TaGS1;2 activity was measured when Glu was supplied at the concentrations 0-5 mM (D). The TaGS1;2 activity was measured at the different concentrations of hydroxylamine when Glu was supplied at the 5mM (E). The volume of individual recombinant wheat GS isozymes crude extract, with 200 μ L of TaGS1;1, 150 μ L of TaGS1;2, 450 μ L of TaGS1;3 and 300 μ L TaGS2 were used for the GS enzyme assays. The relative GS protein content of recombinant wheat GS isozymes crude extract (F). Upper panel showed the TaGS immunoblot and lower panel showed the quantified intensity of the TaGS Western bands present in upper panel. Data represent means \pm SE of at least three replicates.

Fig. 3 TaGS gene expression and GS activity in response to different nitrogen regimes in the shoot and root tissue. Quantitative RT-PCR analysis of TaGS1;1 (A), TaGS1;2 (B), TaGS1;3 (C) and TaGS2 (D) gene expression, horizontal axes present the N absence and the millimolar concentration of NO_3^- and NH_4^+ treatments, vertical axes present the mean relative expression of each isoform normalized to the reference genes *TaATPase* and *TaTEF*. Western-blot analysis of TaGS, TaGS1;1, TaGS1;2, TaGS1;3 and TaGS2 protein contents in shoot (E) and root (F), 15 μ g of soluble proteins extracted from the tissues were loaded onto each lane and detected by the anti-TaGS, anti-TaGS1;1, anti-TaGS1;2, anti-TaGS1;3 and anti-TaGS2 antibody, respectively and the dilution ratio of antibody applied to the membrane is the dilution ratio of antibody is 1:5000, 1:30000, 1:30000,

1:10000 and 1:10000, respectively. Native electrophoresis and in-gel GS activity staining (G) showing the GS holoenzymes in shoot and root; The total GS activity (H) in shoot and root tissue under different N regimes. Data are means of three independent biological replicates \pm SD. The different letters above each sample indicate statistically significant differences where $P < 0.05$ according to one-way ANOVA Duncan post-hoc test.

Fig. 4 Carbon and nitrogen metabolite levels in response to different nitrogen regimes in the shoot and root tissue. The ammonium (A), soluble sugar (B), free amino acid (C) and soluble protein content (D) were determined. Individual amino acid components in response to different nitrogen regimes in the shoot and root tissue. The amino acid components were analyzed with thin layer chromatography (TLC) and ninhydrin colouring showing the amino acid components in shoot (E) and root (G). F showed the separation results of five amino acids (Gln, Ala, Asn, Glu and Asp) under the same conditions. 1.5 μ g of free amino acid extracted from the shoot and root tissues were loaded onto each lane of the TLC. Data are means of three independent biological replicates \pm SD. The different letters above each sample indicate statistically significant differences where $P < 0.05$ according to one-way ANOVA Duncan post-hoc test.

Fig. 5 Tissue localization of individual TaGS. Immunolocalization of TaGS1;1, TaGS1;2, TaGS1;3 and TaGS2 in response to different nitrogen regimes in a transverse section of the leaf (A, D, G), the maturation zone (B, E, H) and meristematic zone (C, F, I) of root tissue. DAPI glowed blue by UV excitation wavelength 330-380 nm and emission wavelength 420 nm; FITC glowed green by excitation wavelength 465-495 nm and emission wavelength 515-555 nm. e, epidermis; MX, metaxylem; P, phloem; X, xylem; VB, vascular bundle; CMX, central metaxylem; End, endodermis; Pr, pericycle; Co, cortex; MC, mesophyll cells.

Fig. 6 Schematic model of individual TaGS1 synergistically perform nitrogen

assimilation and translocation under the condition of N absence (A), NO_3^- supply (B) or NH_4^+ supply (C). V, vessel; St, sieve tube; Cc, phloem companion cells; P, phloem; X, xylem.

Fig. 1

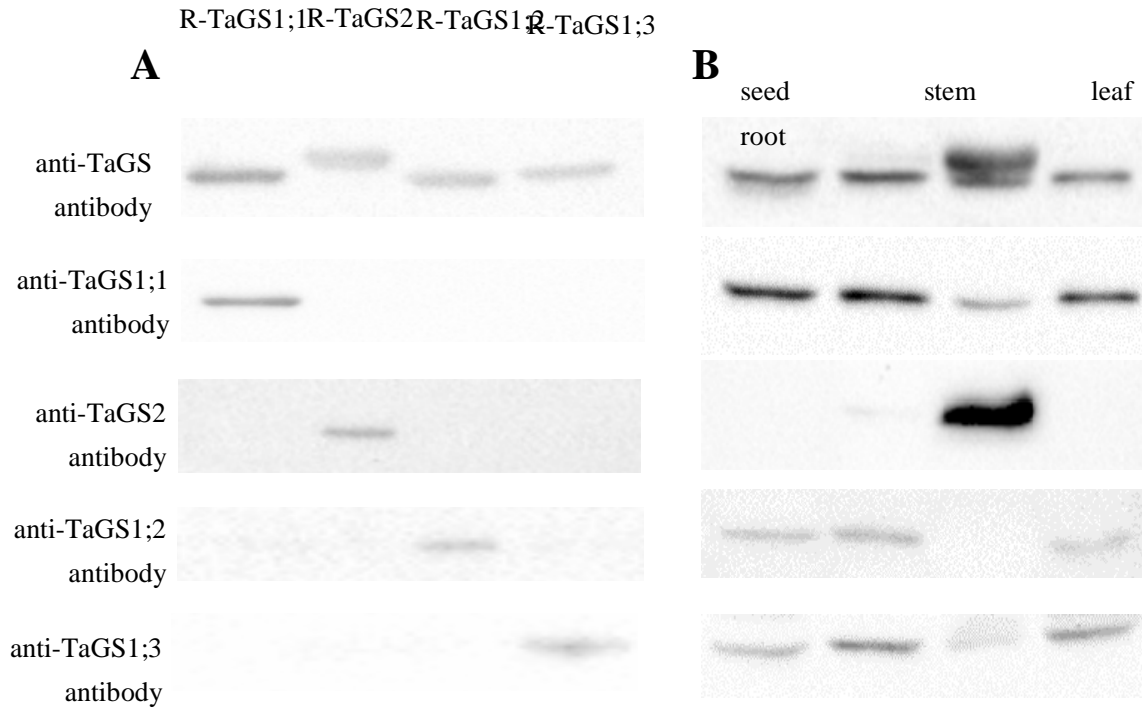


Fig. 2

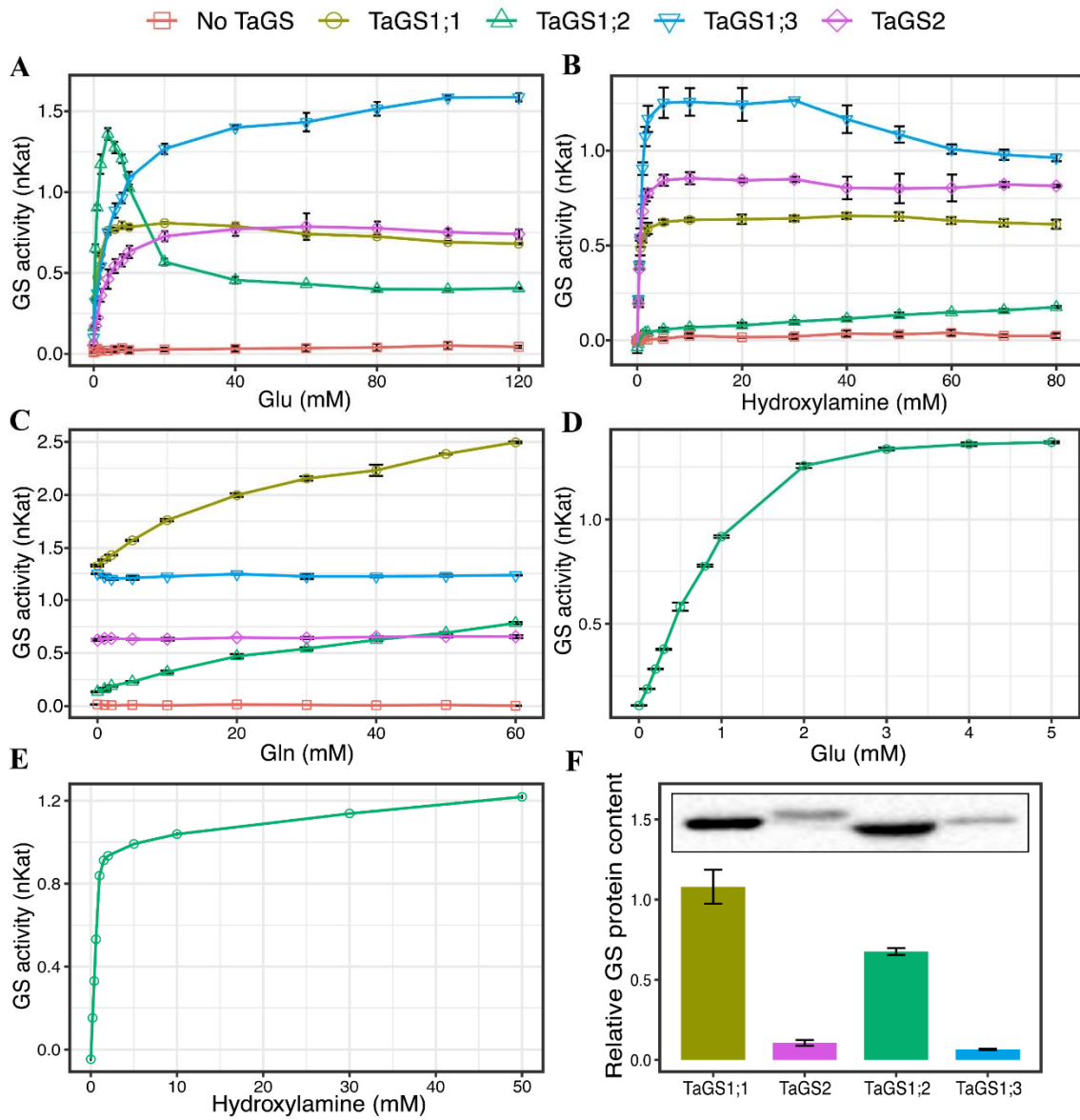


Fig. 3

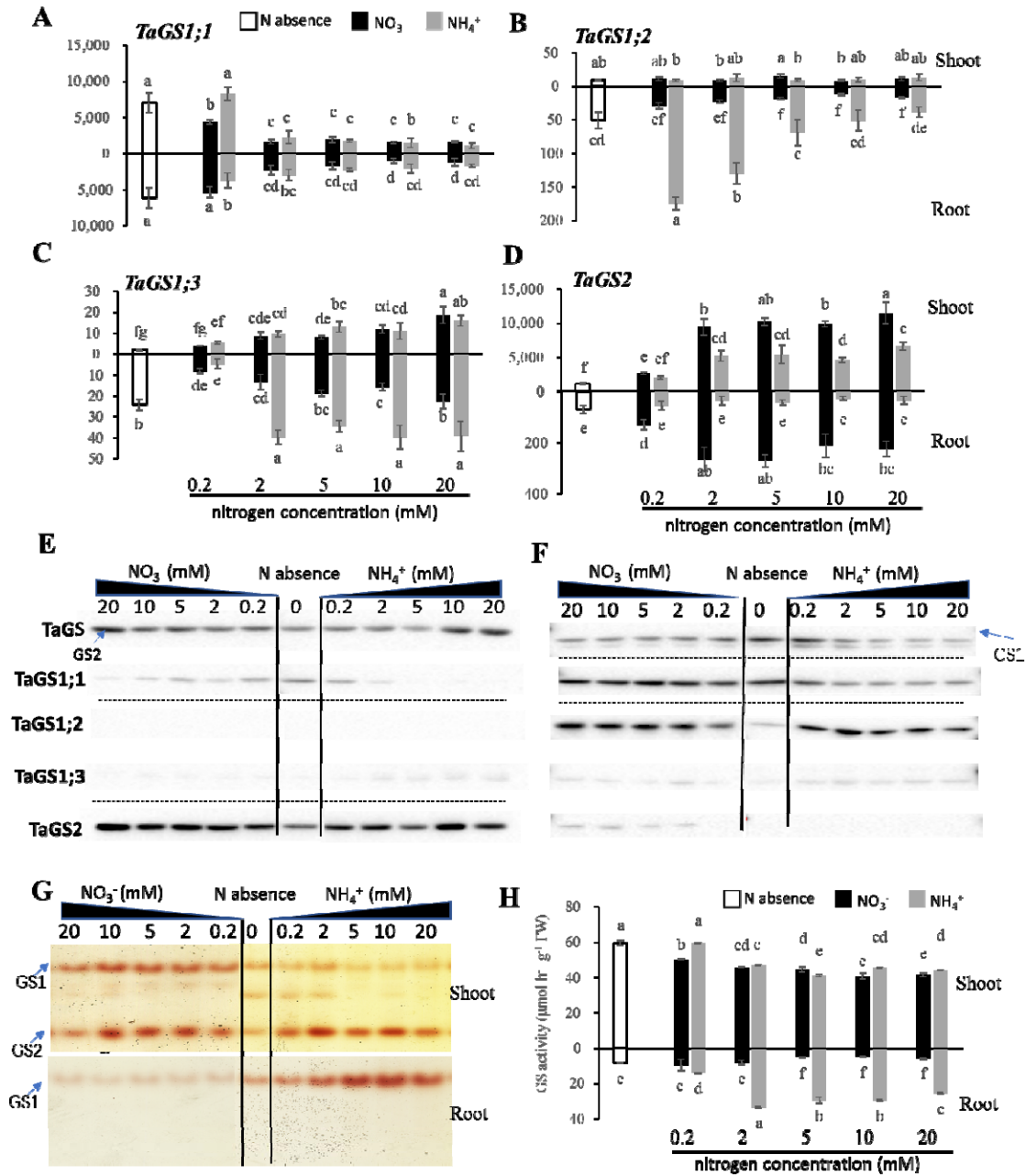


Fig. 4

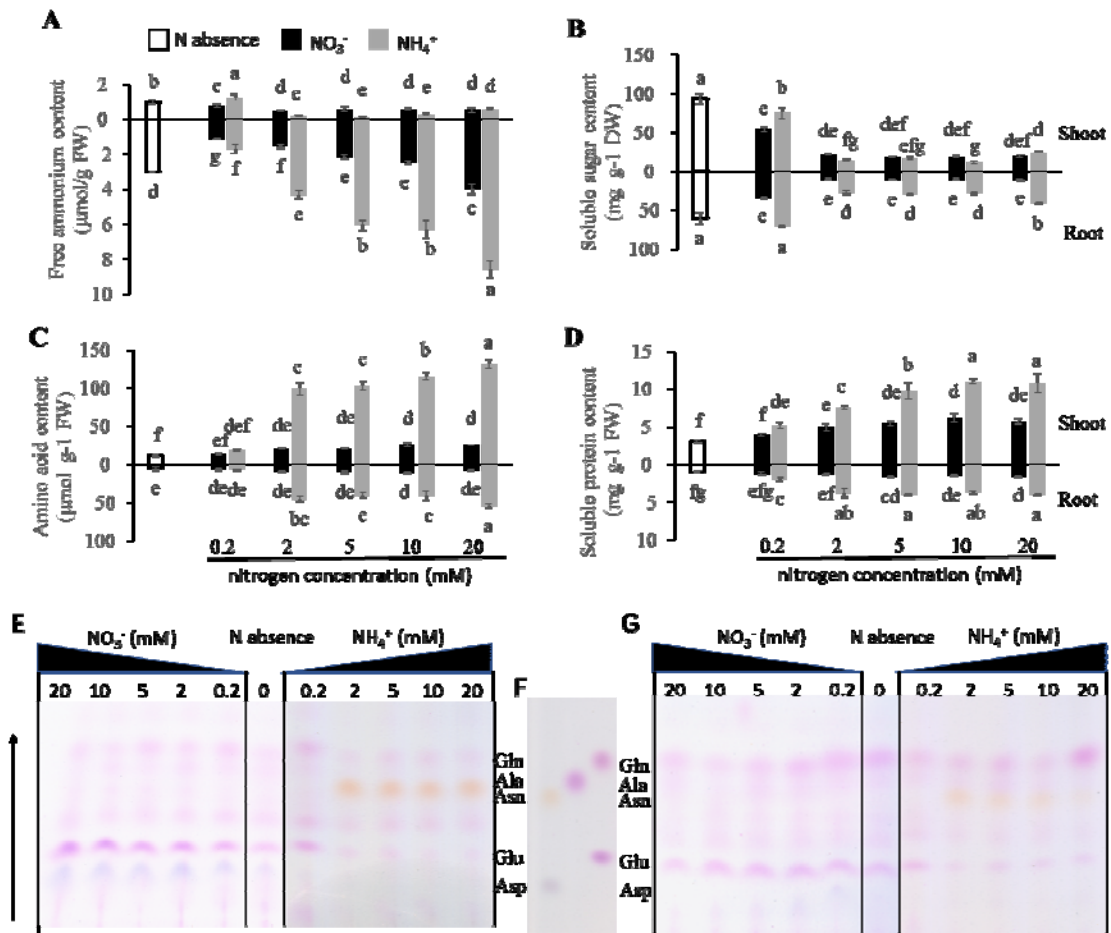


Fig. 5

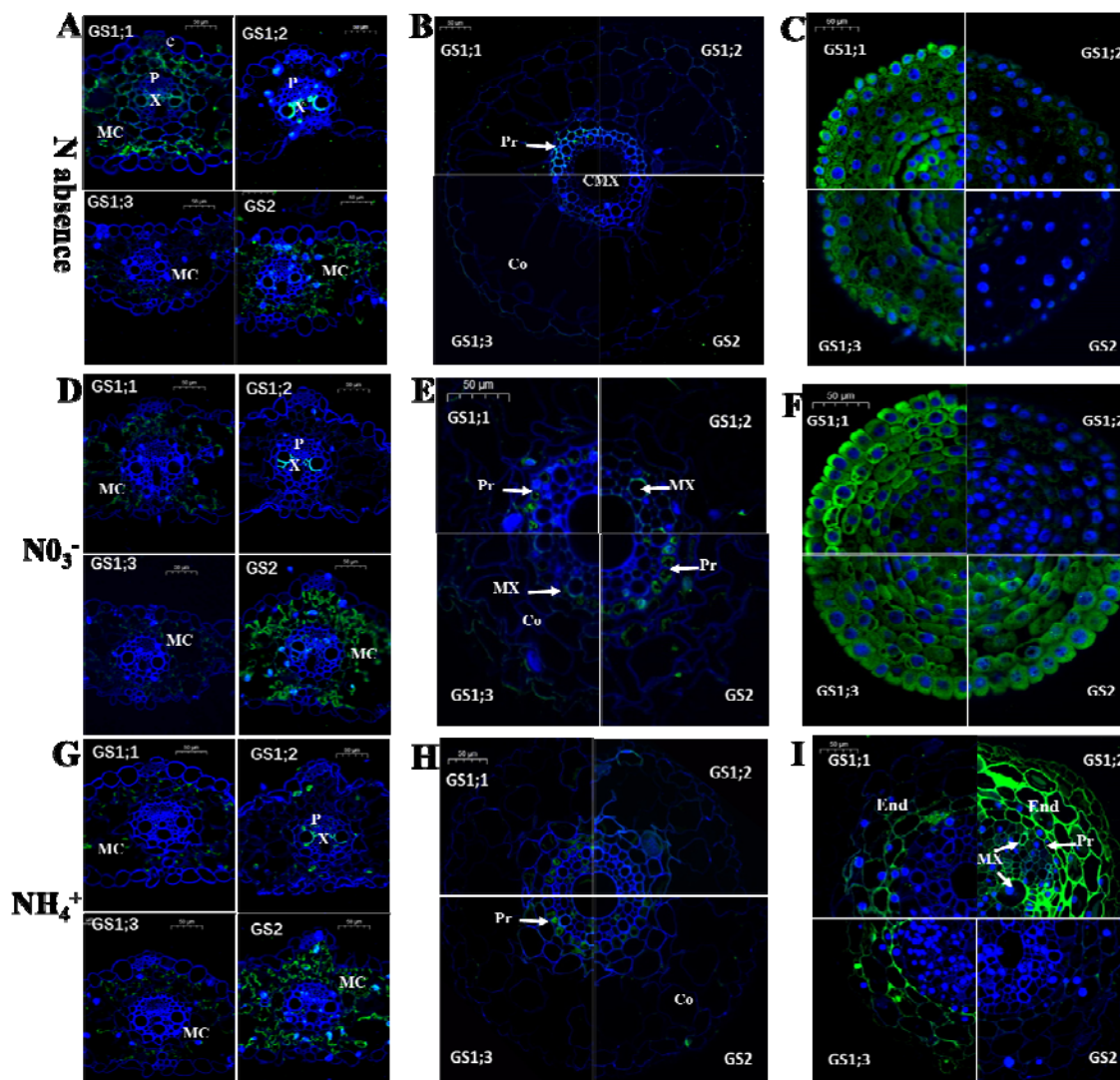


Fig. 6

